Journal of Inflammation Research

Dovepress
open access to scientific and medical research

Open Access Full Text Article

ORIGINAL RESEARCH

Myeloid Cell *Trim59* Deficiency Worsens Experimental Ischemic Stroke and Alters Cerebral Proteomic Profile

Xiang Li[1], Mengtian Pan[1], Xinjuan Tian[1], Lele Zixin Yang[2], Jingjing Zhang[1], Dongmei Yan[3], Baohui Xu[4], Li Zhao[1], Weirong Fang[1]

[1]Department of Physiology, School of Basic Medicine and Clinical Pharmacy, China Pharmaceutical University, Nanjing, Jiangsu, People's Republic of China; [2]The Pennsylvania State University, Eberly College of Science, State College, PA, USA; [3]Department of Immunology, College of Basic Medical Sciences, Jilin University, Changchun, Jilin, People's Republic of China; [4]Department of Surgery, Stanford University School of Medicine, Stanford, CA, USA

Correspondence: Li Zhao; Weirong Fang, Email zhaoli@cpu.edu.cn; weirongfang@cpu.edu.cn

Background: Tripartite motif containing 59 (TRIM59) is a ubiquitin ligase and is involved in the pathogenesis of various diseases, including cancers, sepsis, and other immune-related diseases. However, it has not been defined whether TRIM59 plays a role in ischemic stroke in mice.

Methods: This study determined the influence of *Trim59* deficiency on experimental stroke outcomes and the cerebral proteomic profile using myeloid cell *Trim59* conditional knockout (*Trim59*-cKO) mice and a label-free quantitative proteomic profiling technique. The possible mechanisms by which TRIM59 affected stroke onset were elucidated by in vivo and in vitro experiments.

Results: Immunofluorescence staining results showed that TRIM59 expression was up-regulated after cerebral ischemia and co-localized with macrophages. Myeloid cell *Trim59* deficiency exacerbated ischemic injury on day 3 after experimental stroke. In proteomic analysis, 23 differentially expressed proteins were identified in ischemic brain of *Trim59*-cKO mice as compared to $Trim59^{flox/flox}$ mice. Kyoto Encyclopedia of Genes and Genomes pathway analysis revealed that the differentially expressed proteins were enriched in complement and coagulation cascades. Protein–protein interaction analysis suggested the central role of clusterin in the interaction network. ELISA and Western blot assays confirmed the reduced levels of clusterin protein in the ischemic brains of *Trim59*-cKO mice. Further experimental results showed that clusterin was expressed in neurons. Conditional co-culture experiments of primary neurons and bone marrow-derived macrophages demonstrated that LPS stimulated macrophages to secrete complement C3. In addition, TRIM59 may affect the changes in clusterin expression in an indirect manner by influencing the secretion of complement C3 in macrophages. In vivo experiments also proved a significant increase in C3 levels in the brains of *Trim59*-cKO mice after ischemia.

Conclusion: Myeloid cell *Trim59* deficiency aggravated ischemic stroke outcomes in conjunction with a distinct cerebral proteomic profile, and the underlying mechanism may be related to the regulation of macrophage C3 expression by TRIM59.

Keywords: *Trim59*, ischemic stroke, proteomic profile, complement and coagulation cascades, C3

Introduction

Stroke is one of the most prevalent and devastating diseases worldwide.[1] The 2019 Global Burden of Disease (GBD) Study revealed that there were 12.20 million incident cases of stroke, 101.00 million prevalent cases of stroke, and 6.55 million deaths from stroke in the world,[2] and the data in China were 3.94 million, 28.76 million, and 2.19 million, respectively.[3] In a cross-sectional study of 676,394 participants aged 40 years and older, the overall age-standardized-prevalence, incidence, and mortality rate of stroke in the Chinese mainland were estimated to be 2.61%, 505.2/100,000, and 343.4/100,000, respectively, in the year 2020.[4] Stroke has become the second leading cause of death among rural residents and the third leading cause of death among urban residents in China, posing a significant threat to the health of Chinese citizens.[5] Ischemic stroke is the most common type of stroke, accounting for approximately 87% of cases, and it is caused by occlusion of a major cerebral artery or arterioles.[6,7] In the acute phase, the blood brain barrier is damaged

Received: 14 May 2024
Accepted: 11 July 2024
Published: 19 July 2024

within hours after ischemia,[8] and tight junctions and basement membranes undergo proteolytic degradation within 24 to 48 hours.[9] Subsequently, plasma proteins (including complement) and circulating immune cells migrate into and accumulate in the ischemic lesion.[9] Infiltrating neutrophils and peripheral macrophages in ischemic brain tissue also produce complement that activate the complement cascade reaction.[10]

The complement system can be activated by three pathways: the classical pathway, the alternative pathway, and the lectin pathway, all of which converge on complement C3.[11] C3 is cleaved into two fragments, anaphylatoxin C3a and opsonins C3b, by C3 convertase.[12] C3a recruits and activates immune cells, modulates immune responses, and mediates downstream inflammatory responses.[13] While C3b is mainly involved in opsonization, phagocytosis, and removal of pathogens and cellular debris.[14] The complement system also generates the membrane attack complex, which leads to cell rupture and death.[15] Accumulating evidence suggests that the complement system plays a critical role in the pathogenesis of ischemic brain injury.[13,16] The depletion of complement components or the inhibition of complement activity reduced ischemic brain injury, rescued tissue, and improved functional outcomes in rodent stroke models.[13,17]

In addition to the complement intrinsic components and complement receptors, complement regulatory proteins are important components of the complement system.[18] As a complement regulatory protein, clusterin binds to soluble C5b-9 complement complexes and inhibits cell lysis activity.[19] Clusterin has been shown to attenuate neuroinflammation through its complement-inhibitory properties in Alzheimer's disease[20,21] and stroke.[22,23] Wehrli et al demonstrated that permanent middle cerebral artery occlusion in $Clu^{-/-}$ mice resulted in more ischemic damage than wild type mice.[22] Moreover, clusterin exerts neuroprotective effects in early ischemic events and plays a central role in the remodeling process of ischemic damage.[24]

Tripartite motif (TRIM) proteins are a group of E3 ubiquitin ligases with highly conserved RBCC domains consisting of a RING-finger domain (R), one or two B-box domains (B), and a coiled-coil region (CC).[25,26] TRIM proteins are implicated in innate immunity, development, autophagy, apoptosis, signal transduction and oncogenesis.[26,27] As a ubiquitin ligase[28,29] or an adaptor,[30,31] TRIM59 has been shown to associate with several pathological conditions.[32–36] Meanwhile TRIM59 is inextricably linked to the inflammatory response and complement activation. Myeloid cell TRIM59 protected mice from sepsis by regulating inflammation and phagocytosis.[35] TRIM59 regulated the NRF2/KEAP1 axis pathway by promoting KEAP1 ubiquitin-degradation, thereby ameliorating oxidative stress and the inflammatory response in experimental colitis.[37] In RAW264.7 macrophages, TRIM59 also inhibited complement mediated-phagocytosis.[38] Currently, research on TRIM59 is mainly focused on the field of oncology, such as prostate cancer,[39] pancreatic cancer,[40] lung cancer,[41] and so on. Even fewer studies have been conducted on myeloid cell TRIM59, and its role in ischemic stroke in mice has not been reported. Whether myeloid cell TRIM59 affects the prognosis of ischemic stroke and whether its mechanism is related to the complement system requires further investigation.

In this study, we analyzed the influence of myeloid cell *Trim59* ablation on ischemic stroke outcomes and the cerebral proteomic profile using myeloid cell-specific *Trim59* conditional knockout (*Trim59*-cKO) mice, bioinformatic analyses, and a series of experiments both in vivo and in vitro. The aim of this study is to preliminarily elucidate the intrinsic mechanism by which TRIM59 affects cerebral ischemia, with an outlook of turning TRIM59 into a new target for the treatment of stroke.

Materials and Methods

Mice

Trim59$^{flox/flox}$ mice were obtained from the Cyagen Biosciences Inc. (Guangzhou, Guangdong, China) and cross-bred with myeloid cell-specific Cre transgenic mice (*LysM-Cre*, Jackson Laboratory, Bar Harbor, ME, USA) to generate myeloid cell-specific *Trim59*-cKO mice (Supplementary Figure 1). *Trim59*$^{flox/flox}$ littermates without *LysM-Cre* were used as the controls. All mouse strains were from a C57BL/6N genetic background. Wild type (WT) C57BL/6N mice were purchased from Qinglongshan Animal Breeding Centre (Nanjing, Jiangsu, China). Mice were fed ad libitum at 20–24°C in alternation between day and night. All the experiments were conducted on adult male mice aged 8–10 weeks, weighing 26–30g. The experimental procedures and use of animals were approved by the Ethics Committee of China Pharmaceutical University (approval number: 2021-03-020) and followed the National Institutes of Health Guide for the

Care and Use of Laboratory Animals (https://grants.nih.gov/grants/olaw/Guide-for-the-Care-and-use-of-laboratory-animals.pdf). All experiments were designed and performed according to the Animal Research: Reporting In Vivo Experiments guidelines (https://arriveguidelines.org/). During the surgical procedure, isoflurane was used as anesthesia to ensure the animals did not experience pain. After surgery, the animals' survival status was closely monitored, and euthanasia was performed when the humane endpoint or detection endpoint was reached.

Middle Cerebral Artery Occlusion/Reperfusion (MCAO/R) Surgery

Mice were anesthetized with 3% isoflurane and maintained at 1% to 2% isoflurane; body temperature was maintained at 37 ± 0.5°C with a surface heating pad during the surgery. The right middle cerebral artery was occluded using the intraluminal filament technique as previously described,[42] with minor modification. In brief, the right common carotid artery, external carotid artery, and internal carotid artery were carefully separated. A silicon-coated nylon monofilament (catalog No.0625, Yushun Biotech, Pingdingshan, China) was slowly inserted into the internal carotid artery from the common carotid artery and gently advanced about 10 mm to block the blood supply to the middle cerebral artery. One hour thereafter, the filament was withdrawn for reperfusion. More detailed experimental steps are included in Supplementary Information 1. During the surgery, the cerebral blood flow was measured using the moorFLPI-2 Laser Speckle Contrast Imager (Gene & I, Beijing, China) (Supplementary Figure 2). Additionally, mice were monitored for mortality and body weight after MCAO/R surgery. 18 of 35 *Trim59*$^{flox/flox}$ mice, 18 of 46 *Trim59*-cKO mice, 12 of 19 WT C57BL/6N mice, 6 of 9 Cre-only mice were included for data analysis. The exclusion criteria were as follows: (1) cerebral blood flow dropped less than 70% of the baseline level; (2) no neurological deficits; (3) died within 72 h after the reperfusion; (4) had substantial subarachnoid hemorrhage.

Cell Culture

Mouse bone marrow-derived macrophages (BMDMs) were prepared as described.[35] Briefly, bone marrow cells were removed from the femurs and tibias of 6–8-week old mice and cultured for 7 days in DMEM (KeyGEN, Nanjing, Jiangsu, China) supplemented with 10% fetal bovine serum (Gibco, Grand Island, NY, USA) and 30% conditioned medium from the L929 fibroblast cell line. To establish the inflammatory model, BMDMs were incubated with 200 ng/mL lipopolysaccharide (LPS, Solarbio, Beijing, China) for 12 h.

Primary mice cortical neurons were cultured as described previously,[43] with minor modification. Primary mice cortical neurons were prepared from embryonic-day-18 brains. The cerebral cortices were digested with papain (2mg/mL, Sangon Biotech, Shanghai, China) and DNase solution (0.125mg/mL, Sigma, St. Louis, MO, USA) for 30 min at 37°C. The dissociated neurons were seeded onto six-well plates precoated with cell adhesion agent (Applygen, Beijing, China), and were cultured in Neurobasal medium (Gibco, Grand Island, NY, USA) containing 2% B27 Supplement (Gibco, Grand Island, NY, USA) under 5% CO_2 at 37°C. The medium was renewed every 2 days until the cells appeared in neuronal morphology. The primary neurons were treated with oxygen-glucose deprivation/reoxygenation (OGD/R) to mimic cerebral ischemia/reperfusion injury in vitro.[44] Briefly, Neurobasal medium was replaced with DMEM (KeyGEN, Nanjing, Jiangsu, China) and cells were transferred to a 5% CO_2 and 95% N_2 atmospheric incubator for 2 h at 37°C. After that, neurons were cultured in Neurobasal medium again and maintained in a 5% CO_2 atmospheric incubator for the indicated time periods.

The culture methods for primary mouse microglia and astrocytes are detailed in Supplementary Information 2.

Immunofluorescence Staining

At 72 h after reperfusion, mice were anesthetized and transcardially perfused with 20 mL cold PBS followed by 20 mL 4% polyformaldehyde (Biosharp, Guangzhou, Guangdong, China). Brains were fixed with 4% polyformaldehyde for 72h and then embedded in paraffin to prepare 5-μm sections. For cultured cells, the cells were fixed in 4% polyformaldehyde for 20 min. The brain sections or slides of cells were stained by immunofluorescence using the tyramide signal amplification technique according to the instructions of the fluorescent double-label kit (AiFang biological, Changsha, Hunan, China). The labeling procedure consists of 6 basic steps: (1) sample preparation, (2) blocking of nonspecific epitopes, (3) binding with primary antibody (clusterin, 1:1000, Proteintech Group, Wuhan, Hubei, China; trim59, 1:1000,

Abcam, Cambridge, MA, USA; NeuN, 1:1000, Cell Signaling Technology, Danvers, MA, USA; GFAP,1:1000, Cell Signaling Technology, Danvers, MA, USA; C3, 1:1000, Proteintech Group, Wuhan, Hubei, China), (4) binding with horseradish peroxidase-conjugated secondary antibody, (5) reacting with fluorescent tyramide substrate, and (6) imaging of the signal. More detailed experimental steps can be found in Supplementary Information 3. Stained images were captured by a fluorescent microscope (BX53, Olympus, Tokyo Metropolis, Japan), and analyzed using Image J software (version 1.52v, http://imagej.net).

Evaluation of Infarct Size and Neurological Deficits

Brain infarct size was evaluated at 72 h after MCAO/R. For this purpose, mice were sacrificed under deep anesthesia, and brains were quickly removed and sectioned into five 2-mm-thick coronal sections. All sections were stained with 2% 2, 3, 5-triphenyl-tetrazolium chloride (TTC, Solarbio, Beijing, China) at 37°C for 10 min in the dark, photographed, and analyzed by NIH Image J software (version 1.52v, http://imagej.net). Infarct size was calculated as following: Infarct size(%) =(contralateral area − ipsilateral non infarct area)/contralateral area × 100.[45]

Neurological deficit was assessed using a modified score as previously described:[46] 0 = no observable deficit, 1 = forelimb flexion, 2 = forelimb flexion and decreased resistance to lateral push, 3 = circling, 4 = circling and spinning around the cranial-caudal axis, 5 = no spontaneous movement.

Protein Extraction and Digestion

At 72 h after reperfusion, the mice were deeply anesthetized and euthanized. The brains were rapidly removed and the infarcted hemispheres were isolated. Proteins were quantified using a BCA protein assay kit (Bio-Rad, Hercules, CA, USA), separated on 12.5% SDS-PAGE (20 μg per specimen) at 180V for 45 min, and visualized by Coomassie Blue R-250 staining. Proteins were digested using trypsin according to the filter-aided sample preparation procedure.[47] The resultant peptides were desalted on C18 Cartridges (Empore™ SPE Cartridges C18, Sigma, St. Louis, MO, USA), concentrated by vacuum centrifugation, and reconstituted in 40 μL of 0.1% formic acid.

LC-MS/MS Analysis

Proteolytic peptides were analyzed by LC-MS/MS using a nanoElute liquid chromatography system (Bruker) coupled to a timsTOF Pro mass spectrometer (Bruker). Briefly, peptides were loaded onto a reverse phase trap column (Thermo Scientific Acclaim™ PepMap™ 100, 100 μm × 2 cm, nanoViper C18, Waltham, MA, USA) connected to the C18-reversed phase analytical column (Thermo Scientific Easy Column™, 10 cm long, 75 μm inner diameter, 3 μm resin, Waltham, MA, USA) in 0.1% formic acid and separated with a linear gradient of the buffer containing 84% acetonitrile and 0.1% formic acid at a flow rate of 300 nL/min. A mass spectrometer was operated with positive ion modes to collect ion mobility MS spectra over a mass range of 100–1700 m/z, and 10 cycles of PASEF MS/MS with a target intensity of 1.5k and a threshold of 2500 were subsequently performed. Active exclusion was enabled with a release time of 0.4 min.

Protein Identification and Quantitation

MS raw datasets were analyzed by MaxQuant software (version 1.5.3.17, https://maxquant.net/), the peak lists were searched against the mouse UniProt database (http://www.uniprot.org/) concatenated with a common contaminants database using the parameters listed in Supplementary Table 1.

Bioinformatics Analysis

Major bioinformatic analysis included cluster analysis, subcellular localization, Gene Ontology (GO) annotation, Kyoto Encyclopedia of Genes and Genomes (KEGG) annotation, enrichment analysis, and protein–protein interaction (PPI) analysis.

Cluster 3.0 (http://bonsai.hgc.jp/~mdehoon/software/cluster/software.htm) and Java Treeview software (http://jtreeview.sourceforge.net) were used for hierarchical clustering analysis. The Euclidean distance algorithm was used for similarity measure, and the average linkage clustering algorithm was used for clustering. CELLO (http://cello.life.nctu.edu.tw/), a multi-class SVM classification system, was used to predict protein subcellular localization. The sequences of the selected differentially expressed proteins were locally searched by the NCBI BLAST+ client software (version ncbi-

blast-2.2.28+-win32.exe) and InterProScan (https://www.ebi.ac.uk/interpro/) to find homologue sequences. GO terms were mapped and sequences were annotated using the software program Blast2GO (version 6.0, https://www.blast2go.com/). Following the annotation step, the proteins of interests were blasted against the KEGG database (http://geneontology.org/) to retrieve KEGG ortholog identifications and subsequently be mapped to the pathways. PPI networks for the proteins of interests were analyzed and visualized using STRING (http://string-db.org/) and Cytoscape software (version 3.10.0, http://www.cytoscape.org/). The degree of each protein was further calculated for the assessment of the importance of a given protein in the PPI network.

ELISA and Western Blot Assays

Mice were sacrificed at indicated time points following the MCAO/R surgery. Ischemic brain was mixed with PBS (10 mg tissue/100 μL) and centrifuged at 1000 g for 20 min, and supernatants were collected. Cell culture media supernatants were collected by centrifuging at 1000 g for 20 min. The levels for clusterin (a complement inhibitor) and complement C3 were determined using a commercial ELISA kit (Shanghai Enzyme-linked Biotechnology, Shanghai, China).

For Western blot analysis, total proteins were extracted from the ischemic brains or cultured cells using lysis buffer (Beyotime, Shanghai, China), and protein concentrations were determined by a BCA assay kit (Applygen, Beijing, China). Proteins were separated by SDS-PAGE, transferred onto polyvinylidene fluoride membranes, and incubated with antibodies against clusterin (1:1000, Proteintech Group, Wuhan, Hubei, China), trim59 (1:1000, Abcam, Cambridge, MA, USA) and β-tubulin (1:2000, Affinity Biosciences, Changzhou, Jiangsu, China) at 4°C overnight followed by reaction with goat anti-rabbit IgG conjugated with horseradish peroxidase (1:5000, ABclonal Technology, Wuhan, Hubei, China). The proteins were visualized by an enhanced chemiluminescence detection kit (Applygen, Beijing, China) using the JS-1070 Gel-Pro analyzer (Shanhai Peiqing Science & Technology, Shanghai, China).

Real Time Quantitative Polymerase Chain Reaction (qPCR) Assay

Total RNA was extracted using the RNA isolater (Vazyme, Nanjing, Jiangsu, China). Then, the cDNA was generated using the HiScript II Q RT SuperMix kit (Vazyme, Nanjing, Jiangsu, China) according to manufacturer's instructions. Real time qPCR was performed using ChamQ SYBR qPCR Master Mix kit (Vazyme, Nanjing, Jiangsu, China). The mRNA levels were normalized to β-actin of the same samples and were reported as fold changes relative to control treatment.[48] The primers (Sangon Biotech, Shanghai, China) were as follows:

C3 forward: 5′-AGAAGCGTCTCCATCAAGATTCC-3′
C3 reverse: 5′-ACCACTGTCACGTACTTGTGC-3′
Trim59 forward: 5′-GCTTCTACTGGCATAGAATCCTTAC-3′
Trim59 reverse: 5′-ACATCTGGGTGGTCTTCTTGCT-3′
β-actin forward: 5′-AGAGGGAAATCGTGCGTGAC-3′
β-actin reverse: 5′-CAATAGTGATGACCTGGCCGT-3′

Statistical Analysis

Data were represented as mean ± SEM. IBM SPSS Statistics software (version 19.0) was utilized for all statistical analyses. The differences between two groups were evaluated by Student's *t*-test. Survival rate was tested using the Log Rank test. For neurological function scores and qPCR results, the Mann-Whitney *U*-test was used. A value of $P < 0.05$ was considered statistically significant. To be considered differentially expressed, proteins of *p*-values ≤ 0.05 by Student's *t*-test and a fold change of ≥2 or ≤0.5 in abundance between any two groups were considered significant. Enrichment analysis was based on the Fisher's Exact test. Benjamini-Hochberg correction for multiple testing was further applied to adjust the derived *p*-values. Only functional categories and pathways with *p*-values ≤ 0.05 were considered significant.

Results

TRIM59 Protein Level Increases in Macrophages After Ischemic Injury

We first clarified the changes in TRIM59 expression and the cells in which TRIM59 is predominantly expressed in WT mice after ischemia/reperfusion injury. Under normal physiological conditions, the expression level of TRIM59 in the brains of WT mice is relatively low. With the prolongation of reperfusion time, the expression of TRIM59 protein in the mouse brain showed an upward trend. On the third day after MCAO/R surgery, the expression level of TRIM59 reached its peak (Figure 1A and B). Therefore, this time point was chosen as the detection time point for subsequent indicators. Immunofluorescence results indicated that TRIM59 expression was elevated and mainly expressed on F4/80^{+} cells, not astrocytes and neurons (Figure 1C). Additionally, we cultured primary neurons, microglia, astrocytes, and BMDMs in vitro, and used Western blot experiments to examine the expression of TRIM59 in different cells. The result indicated that TRIM59 was highly expressed in BMDMs (Supplementary Figure 3). An et al demonstrated that TRIM59 is highly expressed in liver, kidney, adipose, testis and lung, but lowly expressed in brain,[49] which is similar to our current experimental results. After cerebral ischemia, the number of F4/80^{+} cells in the mouse brain increased, and the expression of TRIM59 was significantly up-regulated. These results suggested that macrophages might play an essential role in this process.

Myeloid Cell Trim59 Deficiency Aggravates Experimental Ischemic Stroke Outcomes

To identify the role of TRIM59 in macrophages in cerebral ischemia, we generated myeloid cell-specific *Trim59*-cKO mice. Seventy-two hours following the MCAO/R, infarct size was analyzed. No difference was seen in cerebral infarct size among *Trim59*$^{flox/flox}$, Cre-only, and WT C57BL/6N mice, indicating that carrying the *LysM-cre* or *Trim59*-floxed alleles alone did not exacerbate ischemic brain injury in mice (Supplementary Figure 4). *Trim59*$^{flox/flox}$ mice were exclusively used as the control in subsequent experiments. Infarct size was significantly larger in *Trim59*-cKO mice (68.79%) than in *Trim59*$^{flox/flox}$ mice (49.75%) ($P < 0.01$; Figure 2A). As shown in Figure 2B, *Trim59*-cKO mice displayed more severe neurological deficits as compared to *Trim59*$^{flox/flox}$ mice after MCAO/R. Additionally, a trend for reduced body weight was noted in mice after surgery. On the third day after MCAO/R, *Trim59*-cKO mice showed a significant difference in percent body weight change when compared to *Trim59*$^{flox/flox}$ mice (Figure 2C). While mortality was higher in *Trim59*-cKO mice (50%) than in *Trim59*$^{flox/flox}$ mice (75%), the difference did not reach statistical significance (Figure 2D).

Quality Control and Protein Identification

To explore whether the exacerbation of ischemic stroke caused by TRIM59 loss is associated with altered proteomics in ischemic lesion, a label-free approach was used to analyze differentially expressed proteins in the brains between two mouse strains. Among the protein samples that met experimental criteria (Supplementary Table 2 and Supplementary Figure 5), we identified 4,324 proteins from the initial set of 43,271 peptides (Figure 3A). Twenty-three proteins were differentially expressed in two strains of mice following the MCAO/R surgery, with 6 up-regulated (fold change ≥ 2.0, p-value ≤ 0.05) and 17 down-regulated (fold change ≤ 0.5, p-value ≤ 0.05) proteins in the *Trim59*-cKO mice as compared to *Trim59*$^{flox/flox}$ mice (Figure 3B and C, and Table 1).

Subcellular Localization and GO Enrichment Analysis of Differentially Expressed Proteins

Subcellular organelles are specialized structures within which host proteins execute physiological functions. In subcellular localization analysis, 48 (37.2%), 29 (22.5%) and 21 (16.3%) of the differentially expressed proteins were nuclear, extracellular, and cytoplasmic, respectively. Others were located in the plasma membrane, mitochondria and/or other subcellular organelles (Figure 4A).

In GO enrichment analysis, differentially expressed abundant proteins were categorized into biological processes, molecular functions, and cellular components (Figure 4B–D). The rich factor was the ratio of differential proteins to proteins identified in individual categories. More red indicates smaller p-value, demonstrating more reliable and statistical significance in the Fisher's Exact test. Biological processes that were enriched to the highest degree included the inflammatory response,

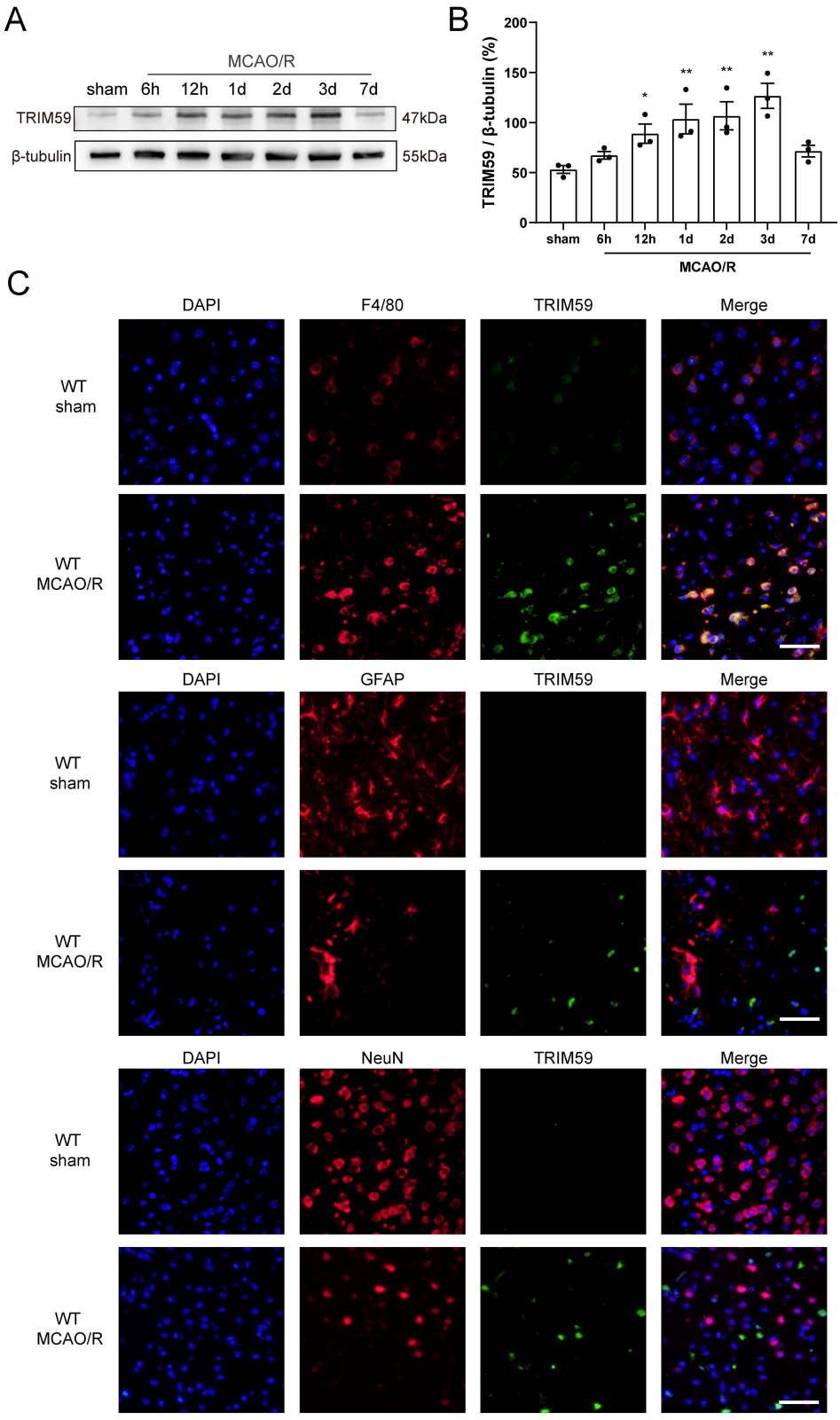

Figure 1 The temporal and spatial expression patterns of TRIM59 in the brains of WT mice after ischemic stroke. (**A** and **B**) Representative Western blot images and quantified data of TRIM59 (n=3). Data are represented as mean ± SEM. *$P < 0.05$, **$P < 0.01$ compared to sham. (**C**) Double immunofluorescence staining of TRIM59. TRIM59 (green) immunoreactive cells are predominantly co-localized with F4/80$^+$ (red), but not NeuN$^+$ (red) or GFAP$^+$ (red) cells in the WT mice brains following ischemia/reperfusion injury. Scale bars, 50 μm.

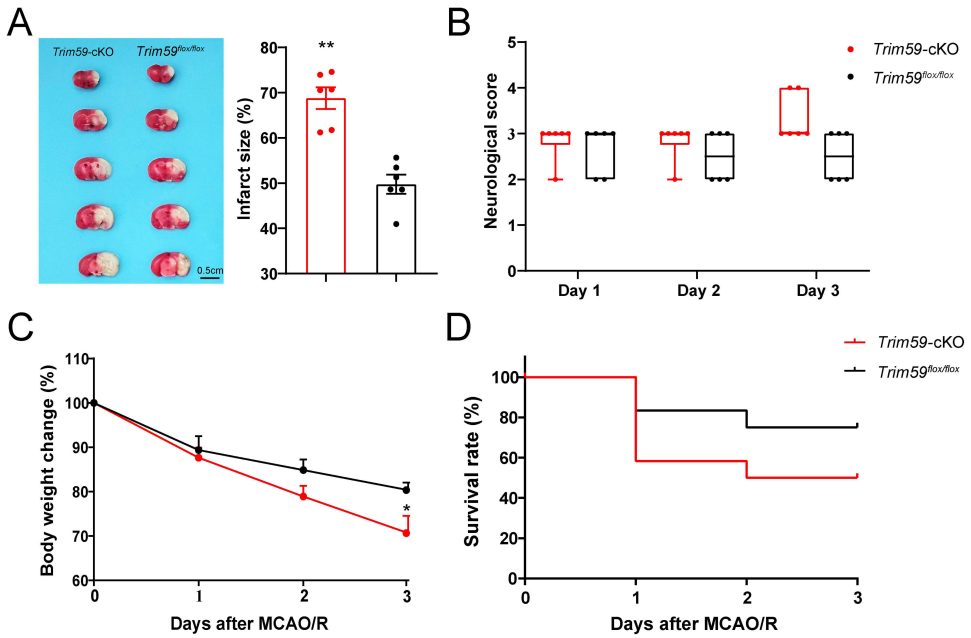

Figure 2 Deletion of myeloid *Trim59* exacerbates ischemic outcomes at 72 h after the MCAO/R. (**A**) Representative TTC staining images and quantification of infarct size. (**B**) Box and whisker plot for neurological score. The horizontal line in each box represents the median. (**C**) Body weight change (%). (**D**) Survival curve. Data are represented as mean ± SEM in A and C. **P* < 0.05, ***P* < 0.01 compared to *Trim59*$^{flox/flox}$ mice. n=6 mice in A-C and 12 mice in D per group.

defense response, protein processing, and others (Figure 4B). These suggested that when macrophages lack *Trim59*, the inflammatory and defensive responses in the brains of stroke mice may be excessively activated, with concomitant effects on protein processing such as protein synthesis, folding, modification, and degradation. Based on molecular functions, differentially expressed proteins were mainly inhibitors to serine-type endopeptidase, peptidase, and other enzymes (Figure 4C). Serine-type endopeptidase and other types of peptidases can catalyze the hydrolysis of proteins and polypeptide chains, playing crucial roles in coagulation and fibrinolytic processes, complement system activation, and inflammatory regulation.[50] In cellular component analysis, the differentially expressed proteins were tightly associated with plasma lipoprotein particle, protein-lipid complex, and extracellular space (Figure 4D). Macrophage TRIM59 may affect lipid metabolism, immune regulation, extracellular signal transduction, and cell–cell interactions after stroke in mice. Thus, TRIM59 may be involved in the regulation of the inflammatory response, complement system activation, and some enzyme inhibitor activity.

KEGG Pathway Enrichment Analysis

In KEGG pathway analysis, differentially expressed proteins were significantly enriched in the complement and coagulation cascades pathway in *Trim59*-cKO mice as compared to *Trim59*$^{flox/flox}$ mice (Figure 5A). In further KEGG pathway enrichment analysis for up-regulated and down-regulated proteins, we also observed that down-regulated proteins were substantially enriched in the same pathway (Figure 5B). The above results suggested that the complement system in the brains of *Trim59*-cKO mice may be in a state of over-activation after stroke onset.

PPI Network Analysis

In the PPI network analysis, we found strong interactions among differentially abundant proteins acting as hubs in the network (Figure 6A). These hub proteins included clusterin (*Clu*), which is involved in lipid transport, cell adhesion, and complement regulation, apolipoprotein A-II (*Apoa2*), which stabilizes high-density lipoprotein structure by its association with lipids and affects the high-density lipoprotein metabolism, and antithrombin-III (*Serpinc1*), which maintains the dynamic homeostasis of the coagulation and anticoagulation systems in the body. Proteins at the center of the PPI network have a higher degree of node connectivity, suggesting that they interact more frequently with other proteins, and may be key targets for TRIM59 to influence the course of ischemic stroke in mice.

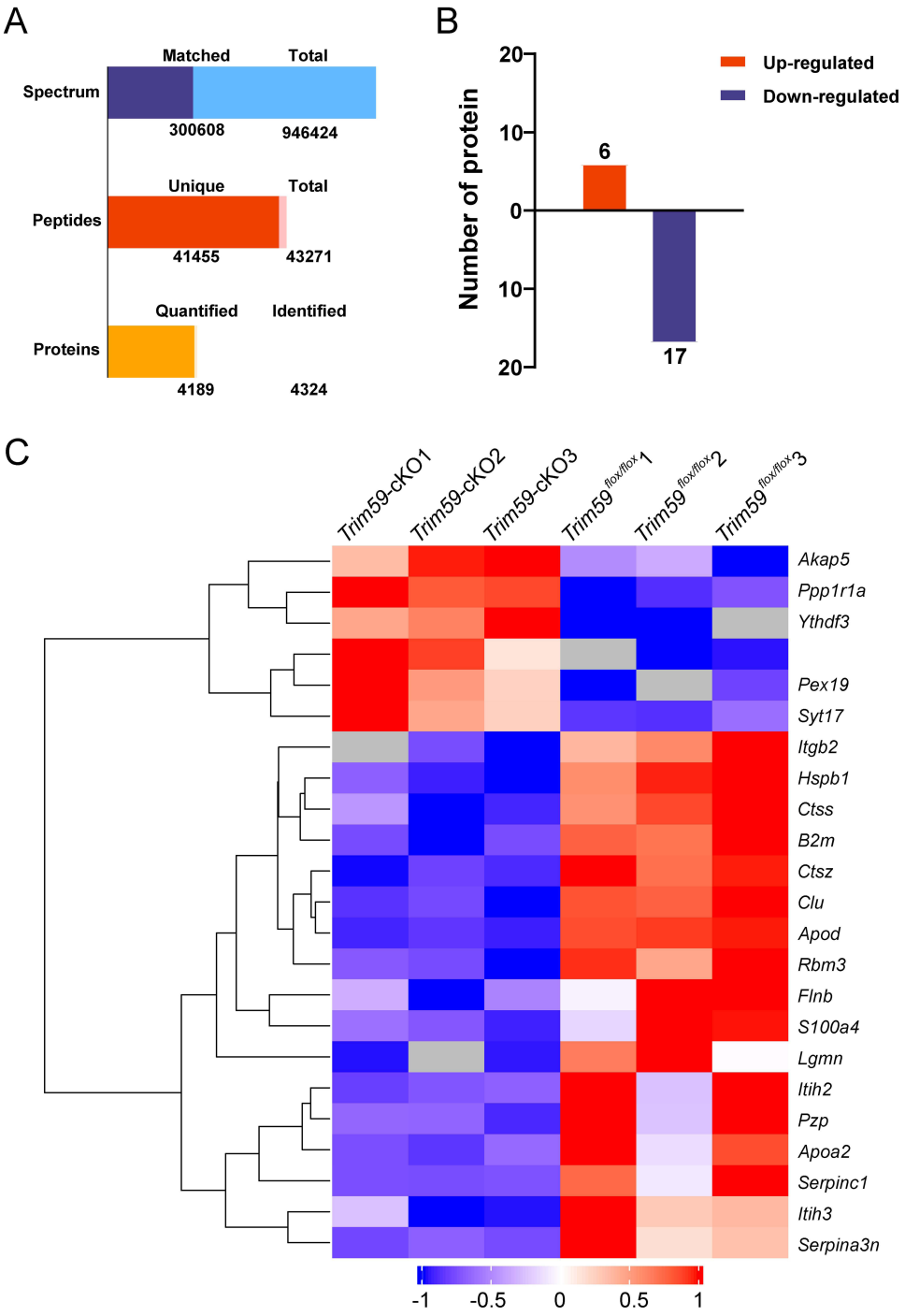

Figure 3 Differential expression of proteins in the brains of *Trim59*-cKO mice and *Trim59*$^{flox/flox}$ mice after the ischemia/reperfusion. (**A**) Numbers of spectrum, peptides, and proteins. Total spectrum: the total number of secondary spectrograms; Matched spectrum: the total number of spectra that matched the database. Total peptides: the total number of peptides; Unique peptides: the total number of unique peptides; Identified Proteins: the total number of identified proteins. Quantified Proteins: the total number of quantifiable proteins. In at least one group, more than half of the biological replicates have an intensity value for this protein. (**B**) Numbers of significantly up-regulated or down-regulated proteins in the brains of *Trim59*-cKO mice in comparison to *Trim59*$^{flox/flox}$ mice (n=3). (**C**) Cluster analysis of differentially expressed proteins in *Trim59*-cKO mice and *Trim59*$^{flox/flox}$ mice following cerebral ischemia/reperfusion. Red: high abundance. Blue: low abundance. Hierarchical clustering was indicated on the left.

Experimental Validation of Differentially Expressed Proteins

In bioinformatics analysis, down-regulated proteins were predominantly enriched in the complement and coagulation cascades pathway. To experimentally validate these findings, we analyzed clusterin levels in the ischemic brains of two mouse strains. In ELISA assay, clusterin levels were significantly reduced in the brains of *Trim59*-cKO mice (765.20 ng/g)

Table 1 Differentially Expressed Proteins in Trim59$^{flox/Flox}$ and Trim59-cKO Mice Following Cerebral Ischemia/Reperfusion

UniProt ID	Protein Name	Gene Name	Fold Change (*Trim59*-cKO/*Trim59*$^{flox/flox}$)	*p*-value
Q8VCI5	Peroxisomal biogenesis factor 19	*Pex19*	2.3060	0.0277
Q8C3W1	Uncharacterized protein C1orf198 homolog		2.2119	0.0170
Q9ERT9	Protein phosphatase 1 regulatory subunit 1A	*Ppp1r1a*	2.1257	0.0001
Q920M7	Synaptotagmin-17	*Syt17*	2.1079	0.0243
D3YVF0	A-kinase anchor protein 5	*Akap5*	2.0119	0.0211
Q8BYK6	YTH domain-containing family protein 3	*Ythdf3*	2.0024	0.0040
O89017	Legumain	*Lgmn*	0.4767	0.0457
O70370	Cathepsin S	*Ctss*	0.4707	0.0036
Q9WUU7	Cathepsin Z	*Ctsz*	0.4665	7.359E-05
Q06890	Clusterin	*Clu*	0.4376	0.0001
Q80X90	Filamin-B	*Flnb*	0.4226	0.0444
P11835	Integrin beta-2	*Itgb2*	0.3860	0.0141
O89086	RNA-binding protein 3	*Rbm3*	0.3679	0.0024
Q61704	Inter-alpha-trypsin inhibitor heavy chain H3	*Itih3*	0.3471	0.0392
P01887	Beta-2-microglobulin	*B2m*	0.3114	0.0008
P07091	Protein S100-A4	*S100a4*	0.2643	0.0374
Q61703	Inter-alpha-trypsin inhibitor heavy chain H2	*Itih2*	0.2500	0.0432
P09813	Apolipoprotein A-II	*Apoa2*	0.2286	0.0395
Q61838	Pregnancy zone protein	*Pzp*	0.2201	0.0449
P14602	Heat shock protein beta-1	*Hspb1*	0.1986	0.0008
P51910	Apolipoprotein D	*Apod*	0.1364	2.225E-06
P32261	Antithrombin-III	*Serpinc1*	0.1084	0.0382
Q91WP6	Serine protease inhibitor A3N	*Serpina3n*	0.0425	0.0412

as compared to *Trim59*$^{flox/flox}$ mice (1247.26 ng/g) after ischemic stroke (Figure 6B, $P < 0.01$). Similar results were further confirmed by Western blot assay (Figure 6C, $P < 0.05$).

LPS-Stimulated Trim59-Deficient Macrophages Suppress Clusterin Expression in Injured Neurons

In WT mice, we found that clusterin was mainly expressed in neurons after cerebral ischemia (Figure 7A). This suggests that TRIM59 may not directly affect clusterin expression in macrophages, but play an indirect regulatory role. Therefore, we cultured primary mouse neurons as well as bone marrow-derived macrophages (BMDMs) in vitro. The BMDMs medium was collected and centrifuged, and the supernatant was taken as the condition medium (CM). The primary mouse neurons were stimulated by CM from different BMDMs (extracted from *Trim59*-cKO mice or *Trim59*$^{flox/flox}$ mice). When primary neurons were in a normal physiological state, the addition of different CM did not result in significant changes of clusterin expression in neurons (Figure 7B). We then performed OGD/R modeling on neurons to mimic in vitro ischemia conditions, and still did not observe differences in the expression of clusterin in the neurons after the addition of different CM (Figure 7C). However, when BMDMs were stimulated with LPS for 12 h and then added the CM to OGD/R-injured neurons, we found obvious differences. After adding the CM of *Trim59*-cKO mice BMDMs, the expression of clusterin in OGD/R treated neurons was significantly reduced (Figure 7D–E, $P < 0.01$). Moreover, we examined the expression of clusterin in different groups of neurons after conditional co-culture using Western blot experiments, and obtained similar results to those of immunofluorescence staining experiments (Figure 7F, $P < 0.05$). LPS stimulation may lead to the secretion of some factors by BMDMs, and the presence of these factors affected the expression of clusterin in neurons. Combining both the proteomics results and the fact that clusterin has a complement-inhibitory function, we hypothesized that these functioning factors may be complement components. However, the specific mechanisms need to be further investigated.

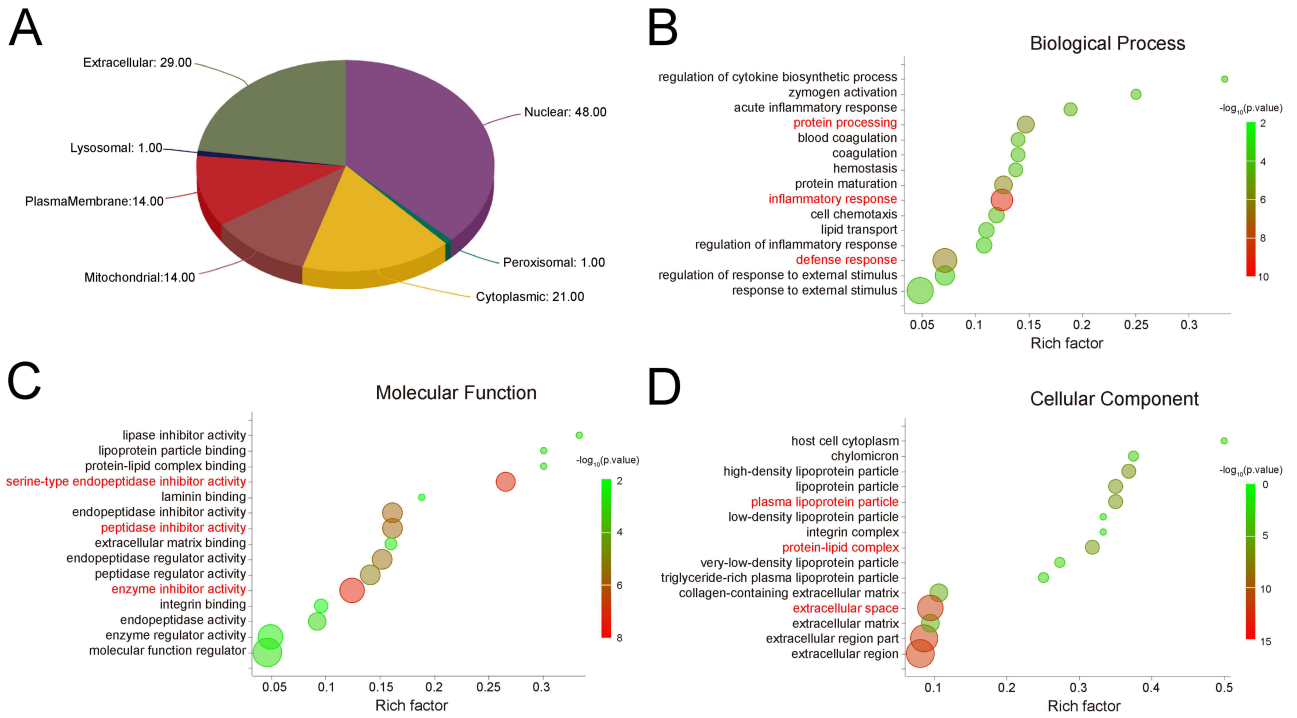

Figure 4 Subcellular localization and GO enrichment analysis of differentially expressed proteins between *Trim59*-cKO mice and *Trim59*$^{flox/flox}$ mice following ischemia/reperfusion injury. (**A**) Subcellular localization. GO analysis of the differentially expressed proteins according to (**B**) Biological Process, (**C**) Molecular Function, and (**D**) Cellular Component. Rich factor: the ratio of differentially expressed proteins to all identified proteins annotated to those individual categories.

Loss of Trim59 in Macrophages Promotes the Expression of Complement C3

First, we stimulated BMDMs with LPS for 12 h in vitro to clarify which factor level was significantly altered. We found that loss of *Trim59* in BMDMs showed a significant increase in the mRNA and protein levels of C3 after LPS stimulation (Figure 8A and B, $P < 0.05$). Subsequently, in vivo ELISA results showed that the expression level of complement C3 in the brains of *Trim59*-cKO mice was significantly higher than that of *Trim59*$^{flox/flox}$ mice on the 3rd day after reperfusion (Figure 8C, $P < 0.01$), and similar results were noted in immunofluorescence staining experiments (Figure 8D and E, $P < 0.01$). At the same time, we discovered that C3 was distributed in the vicinity of F4/80^{+} cells, suggesting that macrophages secreted C3 after infiltrating ischemic brain tissue and macrophages *Trim59* deletion leaded to increased C3 production.

Discussion

In this study, we tentatively believe that the deficiency of *Trim59* in macrophages up-regulated the expression of C3, affected the expression of clusterin in neurons, aggravated the complement-mediated injury of neurons, and further exacerbated ischemic stroke.

Under normal physiological conditions, the expression of TRIM59 is low in mouse brains. On the third day after cerebral ischemia/reperfusion, TRIM59 was extremely increased in the ischemic brain, suggesting that TRIM59 may be an important protein involved in the pathological process of stroke. Immunofluorescence staining experiments and in vitro Western blot experiments showed that TRIM59 was mainly expressed in macrophages. Therefore, we bred *Trim59*-cKO mice, focusing on macrophages, to study the effect of myeloid cell *Trim59* ablation on the development of stroke. Myeloid cell *Trim59* deletion worsened cerebral ischemia/reperfusion injury in the mouse stroke model as evident in increased cerebral infarct size and elevated neurobehavioral scores.

To investigate the potential targets of TRIM59 impacting ischemic stroke, we performed proteomic analysis to identify differentially expressed proteins in ischemic brain of *Trim59*-cKO mice. Label-free quantitative proteomic analysis identified 23 differentially abundant proteins, with 6 up-regulated and 17 down-regulated proteins in *Trim59*-

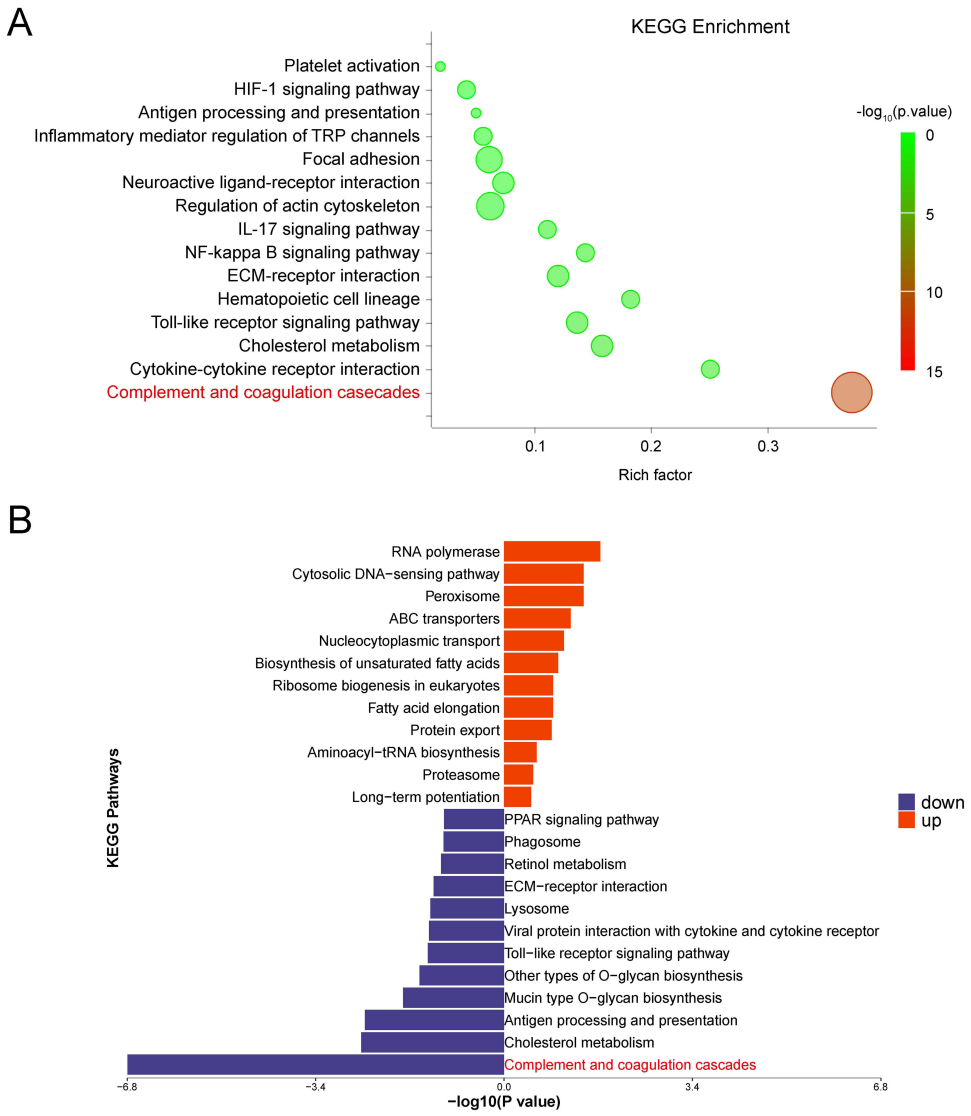

Figure 5 KEGG enrichment analysis of differentially expressed proteins. (**A**) KEGG pathway enrichment bubble plot of differential proteins and (**B**) KEGG pathway enrichment butterfly plot of up- and down-regulated differential proteins. Rich factor: the ratio of differentially expressed proteins to all identified proteins annotated to those individual categories.

cKO mice as compared to *Trim59*$^{flox/flox}$ mice. KEGG enrichment analysis suggested that these differential proteins were predominantly enriched in the complement and coagulation cascades pathway. Complement components are critical in the inflammatory reaction following ischemia and reperfusion.[51] C3 cleavage generates C3a and C3b, and the formation of C5 convertase generates C5a and C5b and aggregates with C6, C7, C8, and C9s to form the membrane attack complex, all of which are implicated in tissue injury following ischemia/reperfusion.[16,52,53] TRIM59 may influence the consequences of cerebral ischemia by modulating a certain link in the complement cascade.

Additionally, the PPI network analysis suggested that clusterin, apolipoprotein A-II, and antithrombin-III contributed to TRIM59-aggravated experimental ischemia/reperfusion injury. Of the three core proteins, clusterin is most closely correlated with the complement pathways.[54] Clusterin, also known as complement lysis inhibitor or apolipoprotein J, is a multifunctional glycoprotein and participates in many biological processes such as cell adhesion, cell membrane restoration, complement system inhibition, sperm maturation, lipid transport, and apoptosis.[55] The overexpression of clusterin by nerve cells was protective against endogenous complement attack following stroke by modulating transforming growth factor-β signaling.[23] Clusterin protein levels were reduced in the brains of *Trim59*-cKO mice as compared to *Trim59*$^{flox/flox}$ mice, suggesting that clusterin may be a potential target protein regulated by TRIM59.

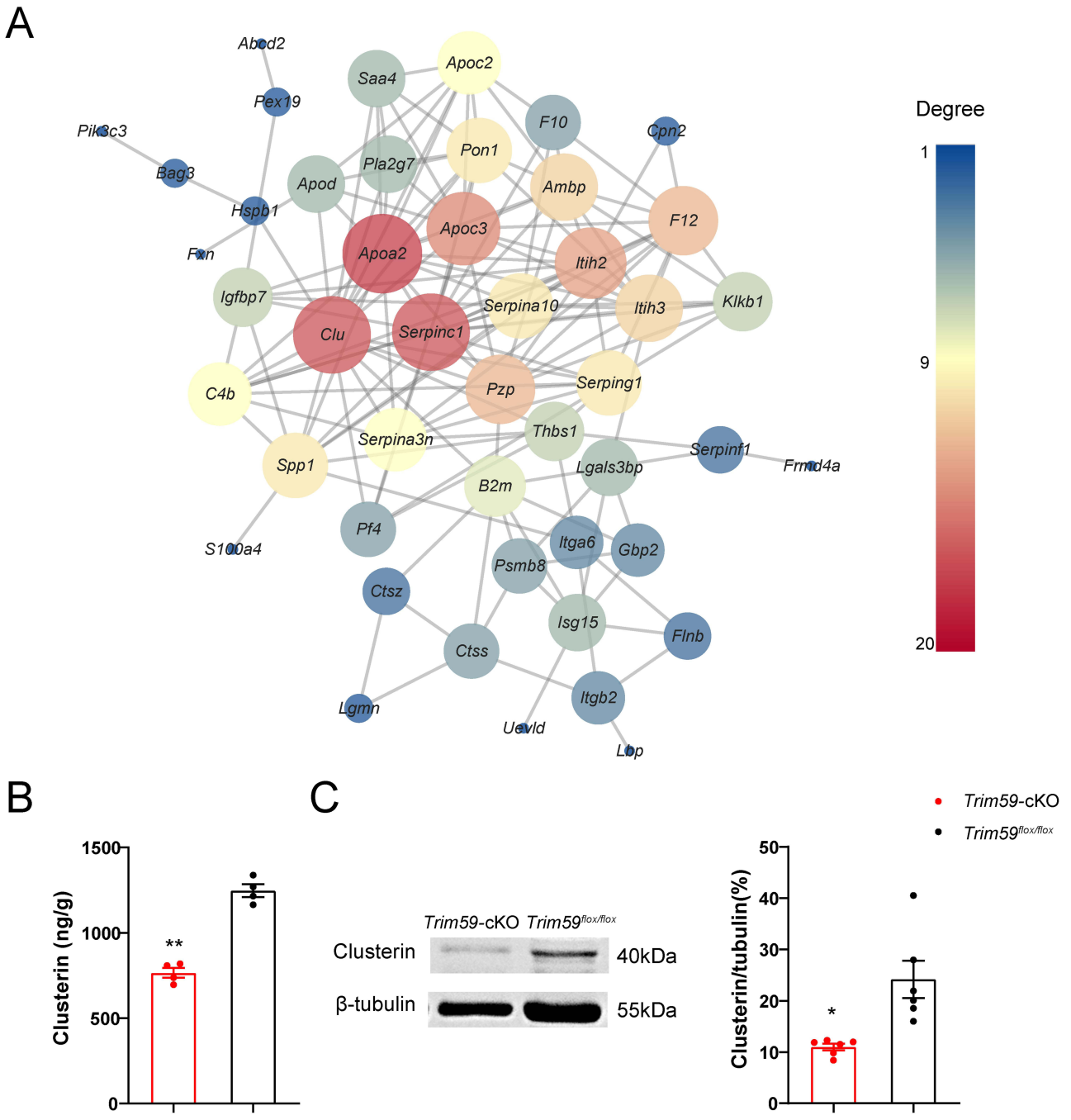

Figure 6 Protein–protein interaction network analysis and validation of differentially expressed proteins. (**A**) Protein–protein interaction network. *Clu*, *Apoa2*, and *Serpinc1* exhibited higher centrality measures than other proteins. Degree: the number of other nodes (proteins) directly connected to this node. *Trim59*-cKO mice and *Trim59*$^{flox/flox}$ mice underwent MCAO/R injury, and ischemic brain tissue was collected at 72 h after the surgery. (**B**) The levels of clusterin determined by ELISA (n=4). (**C**) Representative Western blot images and quantified data of clusterin (n=6). Data are represented as mean ± SEM. *$P < 0.05$, **$P < 0.01$ compared to *Trim59*$^{flox/flox}$ mice.

However, the subsequent experimental results revised our initial assumption. TRIM59 could hardly exert a direct regulatory effect on clusterin due to the difference in the cells where TRIM59 and clusterin are mainly expressed (TRIM59 in macrophages and clusterin in neurons). We turned our attention back to the complement pathway to find the mediator between the two. Conditional co-culture experiments with primary neurons and BMDMs showed that LPS stimulated BMDMs to secrete a certain factor that affected neuronal clusterin expression. Further in vitro experiments demonstrated that *Trim59*-deficient macrophages produce more complement C3 after LPS treatment. These were also

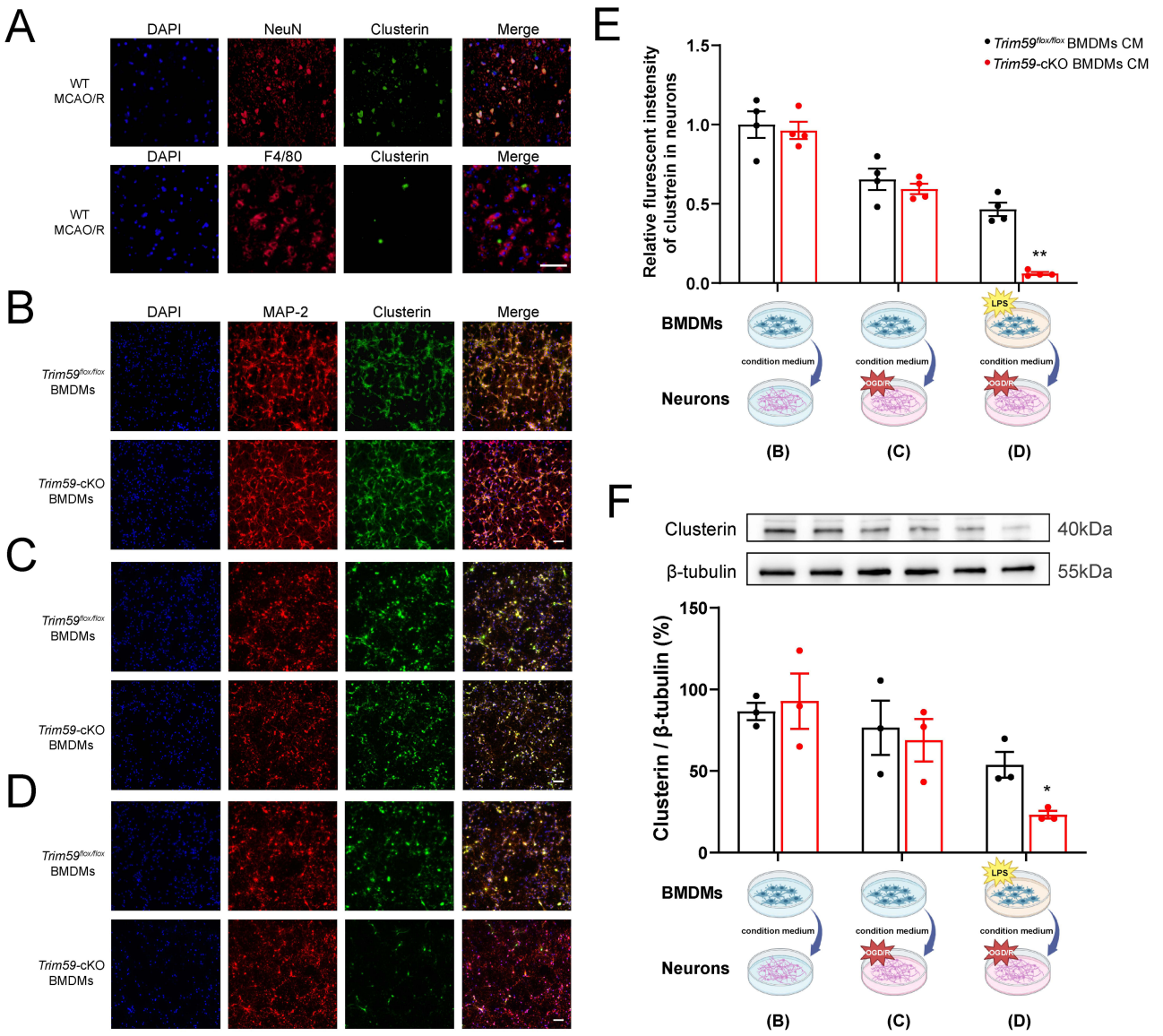

Figure 7 Clusterin is mainly expressed in neurons in WT mice brain after cerebral ischemia. Primary neurons (MAP-2^{+}, red) stimulated by different BMDMs condition medium (CM) can induce changes in clusterin (green) expression. Scale bars, 50 μm. (**A**) Clusterin (green) immunoreactive cells are mainly co-localized with NeuN (red), not F4/80 (red) in WT mice brain. (**B**) Normal primary neurons stimulated by normal BMDMs CM. (**C**) OGD/R-treated neurons stimulated by normal BMDMs CM. (**D**) OGD/R-treated neurons stimulated by LPS-injured BMDMs CM. (**E**) Quantification of clusterin expression in primary neurons (n=4). (**F**) Representative Western blot images and quantified data of clusterin in primary neurons (n=3). Data are represented as mean ± SEM. *P < 0.05, **P < 0.01 compared to *Trim59*$^{flox/flox}$ BMDMs CM.

supported by in vivo experiments with higher levels of C3 in the brains of *Trim59*-cKO mice after MCAO/R surgery. In summary, TRIM59 may affect neuronal clusterin expression by influencing the secretion of C3 in macrophages, and impact neuronal damage mediated by complement. After the onset of cerebral ischemia, the elevated levels of C3 in the brains of *Trim59*-cKO mice were accompanied by reduced levels of clusterin, and the superposition of the two results caused the *Trim59*-cKO mice to develop more severe ischemic brain injury.

There are several limitations to our study. Firstly, the role of other myeloid cells, such as neutrophils, in cerebral ischemia has not been studied in detail. We only explained the possible mechanism by which myeloid cell knockout of *Trim59* worsened brain injury from the perspective of macrophages. Secondly, how C3 specifically affected the expression of clusterin was not addressed in this study, and further experiments are needed for in-depth study. Thirdly, proteomics technology has certain limitations in detecting membrane proteins. Their hydrophobic transmembrane regions and the complexity of their own structure result in poor solubility and make them less amenable to detection. Recently,

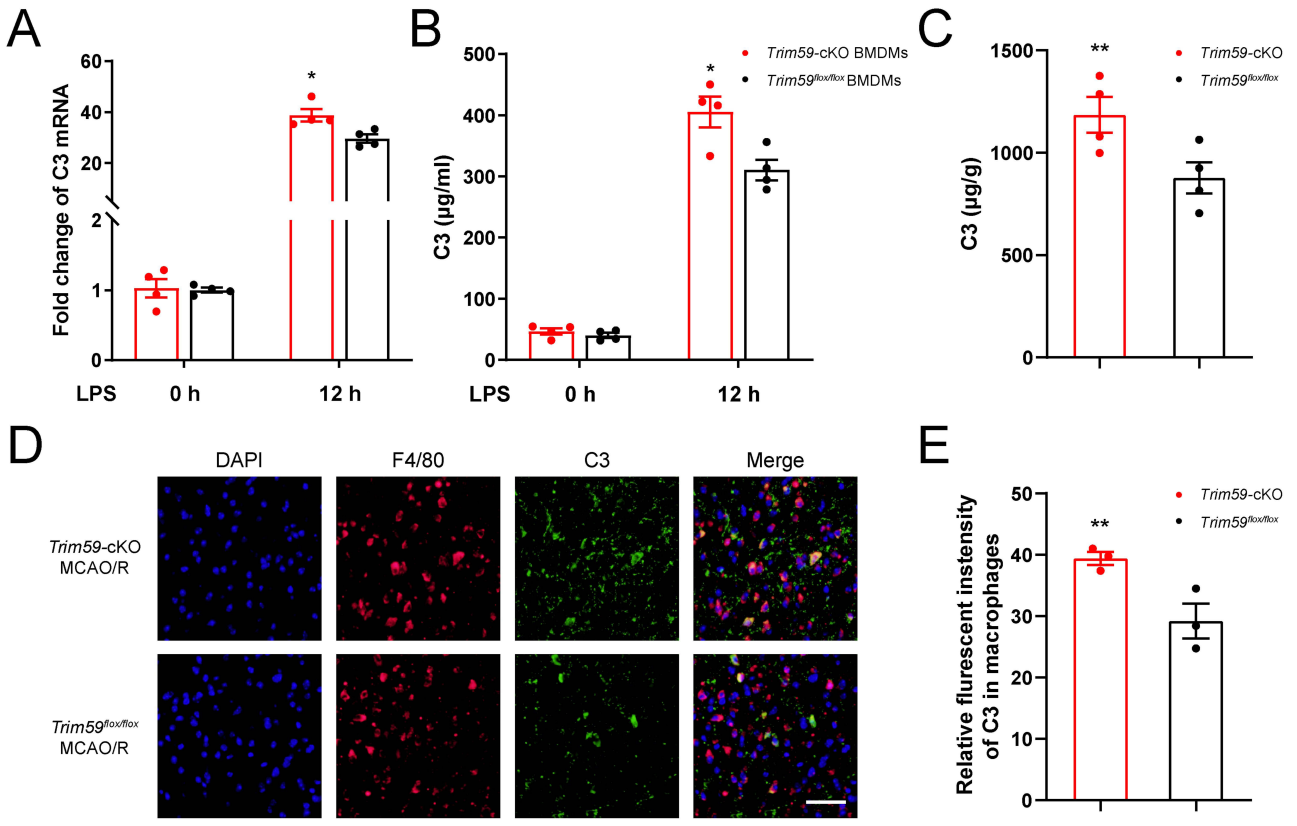

Figure 8 Loss of *Trim59* in macrophages promotes the expression of complement C3. (**A** and **B**) The mRNA and protein levels of C3 in BMDMs after LPS stimulation for 12 h were determined by qPCR and ELISA (n=4). Data are represented as mean ± SEM. **P* < 0.05 compared to *Trim59*$^{flox/flox}$ BMDMs. (**C**) The level of C3 in ischemic brain of mice was determined by ELISA (n=4). (**D**) Double immunofluorescence staining of F4/80 (red) and C3 (green) in ischemic brain of mice at 72 h post-MCAO/R. Scale bars, 50 μm. (**E**) Quantification of C3 expression in macrophages (n=3). Data are represented as mean ± SEM. ***P* < 0.01 compared to *Trim59*$^{flox/flox}$ mice.

two members of the transient receptor potential melastatin (TRPM) channel family, TRPM2 and TRPM4, were shown to be involved in N-methyl-D-aspartate receptors-mediated excitotoxicity during ischemic stroke.[56] We did not detect data related to TRPM2 and TRPM4 in our proteomics sequencing results, which also suggests that the differences in protein expression in the brains of stroke mice caused by TRIM59 may not be limited to the results shown in this study.

In conclusion, the present study found that myeloid cell *Trim59* deficiency aggregated experimental ischemic stroke outcomes in association with an altered cerebral proteomic pattern. Mechanistically, TRIM59 affects post-ischemic injury by regulating macrophage C3 expression. Our findings may provide new insights to the study of the role of TRIM59 in ischemic stroke.

Abbreviations

CM, condition medium; GO, Gene Ontology; KEGG, Kyoto Encyclopedia of Genes and Genomes; MCAO/R, middle cerebral artery occlusion/reperfusion; OGD/R, oxygen-glucose deprivation/reoxygenation; PPI, protein–protein interaction; TRIM59, tripartite motif containing 59; *Trim59*-cKO, myeloid cell *Trim59* conditional knockout; WT, wild type.

Data Sharing Statement

All datasets are available from the corresponding author upon reasonable request. The mass spectrometry proteomics data have been deposited to the ProteomeXchange Consortium via the PRIDE partner repository with the dataset identifier PXD049258.

Funding

This work was supported by the Natural Science Foundation of China (grant numbers 82174051 and 82073845).

Disclosure

All authors declare no conflicts of interest in this work.

References

1. Collaborators GBDS. Global, regional, and national burden of stroke, 1990–2016: a systematic analysis for the Global Burden of Disease Study 2016. *Lancet Neurol*. 2019;18(5):439–458. doi:10.1016/S1474-4422(19)30034-1
2. GBD 2019 Stroke Collaborators. Global, regional, and national burden of stroke and its risk factors, 1990–2019: a systematic analysis for the Global Burden of Disease Study 2019. *Lancet Neurol*. 2021;20(10):795–820. doi:10.1016/s1474-4422(21)00252-0
3. Ma Q, Li R, Wang L, et al. Temporal trend and attributable risk factors of stroke burden in China, 1990–2019: an analysis for the Global Burden of Disease Study 2019. *Lancet Public Health*. 2021;6(12):e897–e906. doi:10.1016/s2468-2667(21)00228-0
4. Tu WJ, Zhao Z, Yin P, et al. Estimated burden of stroke in China in 2020. *JAMA network open*. 2023;6(3):e231455. doi:10.1001/jamanetworkopen.2023.1455
5. Tu WJ, Wang LD. China stroke surveillance report 2021. *Military Med Res*. 2023;10(1):33. doi:10.1186/s40779-023-00463-x
6. Tsao CW, Aday AW, Almarzooq ZI, et al. Heart disease and stroke statistics-2022 update: a report from the American Heart Association. *Circulation*. 2022;145(8):e153–e639. doi:10.1161/CIR.0000000000001052
7. Iadecola C, Buckwalter MS, Anrather J. Immune responses to stroke: mechanisms, modulation, and therapeutic potential. *J Clin Investig*. 2020;130(6):2777–2788. doi:10.1172/JCI135530
8. Knowland D, Arac A, Sekiguchi KJ, et al. Stepwise recruitment of transcellular and paracellular pathways underlies blood-brain barrier breakdown in stroke. *Neuron*. 2014;82(3):603–617. doi:10.1016/j.neuron.2014.03.003
9. Yang Y, Rosenberg GA. Blood-brain barrier breakdown in acute and chronic cerebrovascular disease. *Stroke*. 2011;42(11):3323–3328. doi:10.1161/STROKEAHA.110.608257
10. Alsbrook DL, Di Napoli M, Bhatia K, et al. Neuroinflammation in Acute Ischemic and Hemorrhagic Stroke. *Curr Neurol Neurosci Rep*. 2023;23(8):407–431. doi:10.1007/s11910-023-01282-2
11. Bohlson SS, Tenner AJ. Complement in the brain: contributions to neuroprotection, neuronal plasticity, and neuroinflammation. *Ann Rev Immunol*. 2023;41:431–452. doi:10.1146/annurev-immunol-101921-035639
12. Veerhuis R, Nielsen HM, Tenner AJ. Complement in the brain. *Mol Immunol*. 2011;48(14):1592–1603. doi:10.1016/j.molimm.2011.04.003
13. Ma Y, Liu Y, Zhang Z, Yang GY. Significance of Complement System in Ischemic Stroke: a Comprehensive Review. *Aging Dis*. 2019;10(2):429–462. doi:10.14336/ad.2019.0119
14. Dalakas MC, Alexopoulos H, Spaeth PJ. Complement in neurological disorders and emerging complement-targeted therapeutics. *Nat Rev Neurol*. 2020;16(11):601–617. doi:10.1038/s41582-020-0400-0
15. Ling M, Murali M. Analysis of the Complement System in the Clinical Immunology Laboratory. *Clinics Lab Med*. 2019;39(4):579–590. doi:10.1016/j.cll.2019.07.006
16. Clarke AR, Christophe BR, Khahera A, Sim JL, Connolly ES. Therapeutic modulation of the complement cascade in stroke. *Front Immunol*. 2019;10:1723. doi:10.3389/fimmu.2019.01723
17. Ducruet AF, Zacharia BE, Sosunov SA, et al. Complement inhibition promotes endogenous neurogenesis and sustained anti-inflammatory neuroprotection following reperfused stroke. *PLoS One*. 2012;7(6):e38664. doi:10.1371/journal.pone.0038664
18. Jiang Y, Liu Z, Liao Y, Sun S, Dai Y, Tang Y. Ischemic stroke: from pathological mechanisms to neuroprotective strategies. *Front Neurol*. 2022;13:1013083. doi:10.3389/fneur.2022.1013083
19. Barnum SR, Bubeck D, Schein TN. Soluble membrane attack complex: biochemistry and immunobiology. *Front Immunol*. 2020;11:585108. doi:10.3389/fimmu.2020.585108
20. Yuste-Checa P, Bracher A, Hartl FU. The chaperone Clusterin in neurodegeneration-friend or foe? *BioEssays*. 2022;44(7):e2100287. doi:10.1002/bies.202100287
21. De Miguel Z, Khoury N, Betley MJ, et al. Exercise plasma boosts memory and dampens brain inflammation via clusterin. *Nature*. 2021;600(7889):494–499. doi:10.1038/s41586-021-04183-x
22. Wehrli P, Charnay Y, Vallet P, et al. Inhibition of post-ischemic brain injury by clusterin overexpression. *Nature Med*. 2001;7(9):977–979. doi:10.1038/nm0901-977
23. Charnay Y, Imhof A, Vallet PG, Kovari E, Bouras C, Giannakopoulos P. Clusterin in neurological disorders: molecular perspectives and clinical relevance. *Brain Res Bull*. 2012;88(5):434–443. doi:10.1016/j.brainresbull.2012.05.006
24. Imhof A, Charnay Y, Vallet PG, et al. Sustained astrocytic clusterin expression improves remodeling after brain ischemia. *Neurobiol Dis*. 2006;22(2):274–283. doi:10.1016/j.nbd.2005.11.009
25. Lu K, Pan Y, Huang Z, Liang H, Ding ZY, Zhang B. TRIM proteins in hepatocellular carcinoma. *J Biomed Sci*. 2022;29(1):69. doi:10.1186/s12929-022-00854-7
26. Hatakeyama S. TRIM family proteins: roles in autophagy, immunity, and carcinogenesis. *Trends Biochem Sci*. 2017;42(4):297–311. doi:10.1016/j.tibs.2017.01.002
27. van Gent M, Sparrer KMJ, Gack MU. TRIM proteins and their roles in antiviral host defenses. *Ann Rev Virol*. 2018;5(1):385–405. doi:10.1146/annurev-virology-092917-043323
28. Wang F, Wang H, Sun L, Niu C, Xu J. TRIM59 inhibits PPM1A through ubiquitination and activates TGF-beta/Smad signaling to promote the invasion of ectopic endometrial stromal cells in endometriosis. *Am J Physiol Cell Physiol*. 2020;319(2):C392–C401. doi:10.1152/ajpcell.00127.2019
29. Han T, Guo M, Gan M, Yu B, Tian X, Wang JB. TRIM59 regulates autophagy through modulating both the transcription and the ubiquitination of BECN1. *Autophagy*. 2018;14(12):2035–2048. doi:10.1080/15548627.2018.1491493
30. Kondo T, Watanabe M, Hatakeyama S. TRIM59 interacts with ECSIT and negatively regulates NF-kappaB and IRF-3/7-mediated signal pathways. *Biochem Biophys Res Commun*. 2012;422(3):501–507. doi:10.1016/j.bbrc.2012.05.028

31. Xu G, Ma Z, Yang F, et al. TRIM59 promotes osteosarcoma progression via activation of STAT3. *Human Cell*. 2022;35(1):250–259. doi:10.1007/s13577-021-00615-y
32. Chen G, Chen W, Ye M, Tan W, Jia B. TRIM59 knockdown inhibits cell proliferation by down-regulating the Wnt/beta-catenin signaling pathway in neuroblastoma. *Biosci Rep*. 2019;39(1). doi:10.1042/BSR20181277
33. Zhang JN, Ding DY, Yang SY, Tao QF, Yang Y, Zhou WP. The role of Tripartite motif containing 59 (TRIM59) in the proliferation and prognosis of intrahepatic cholangiocarcinoma. *Pathol Res Pract*. 2022;236:153989. doi:10.1016/j.prp.2022.153989
34. Lv ZQ, Yang CY, Xing QS. TRIM59 attenuates inflammation and apoptosis caused by myocardial ischemia reperfusion injury by activating the PI3K/Akt signaling pathway. *Eur Rev Med Pharmacol Sci*. 2020;24(7):4005–4015. doi:10.26355/eurrev_202004_20870
35. Jin Z, Zhu Z, Liu S, et al. TRIM59 protects mice from sepsis by regulating inflammation and phagocytosis in macrophages. *Front Immunol*. 2020;11:263. doi:10.3389/fimmu.2020.00263
36. Jin Z, Chen T, Zhu Z, Xu B, Yan D. The role of TRIM59 in immunity and immune-related diseases. *Int Rev Immunol*. 2022;1–8. doi:10.1080/08830185.2022.2102618
37. Liu B, Gao Y, Liu X, Lian Q, Li Y. Tripartite motif containing 59 mediates protective anti-oxidative effects in intestinal injury through Nrf2 signaling. *Int Immunopharmacol*. 2023;124(Pt B):110896. doi:10.1016/j.intimp.2023.110896
38. Jin Z, Zhu Z, Zhang W, et al. Effects of TRIM59 on RAW264.7 macrophage gene expression and function. *Immunobiology*. 2021;226(4):152109. doi:10.1016/j.imbio.2021.152109
39. Fan L, Gong Y, He Y, et al. TRIM59 is suppressed by androgen receptor and acts to promote lineage plasticity and treatment-induced neuroendocrine differentiation in prostate cancer. *Oncogene*. 2023;42(8):559–571. doi:10.1038/s41388-022-02498-1
40. Che B, Du Y, Yuan R, et al. SLC35F2-SYVN1-TRIM59 axis critically regulates ferroptosis of pancreatic cancer cells by inhibiting endogenous p53. *Oncogene*. 2023;42(44):3260–3273. doi:10.1038/s41388-023-02843-y
41. Liang M, Chen X, Wang L, et al. Cancer-derived exosomal TRIM59 regulates macrophage NLRP3 inflammasome activation to promote lung cancer progression. *J Exp Clin Cancer Res*. 2020;39(1):176. doi:10.1186/s13046-020-01688-7
42. Fang W, Zhai X, Han D, et al. CCR2-dependent monocytes/macrophages exacerbate acute brain injury but promote functional recovery after ischemic stroke in mice. *Theranostics*. 2018;8(13):3530–3543. doi:10.7150/thno.24475
43. Rubiolo JA, Vale C, Boente-Juncal A, et al. Transcriptomic analysis of ciguatoxin-induced changes in gene expression in primary cultures of mice cortical neurons. *Toxins*. 2018;10(5). doi:10.3390/toxins10050192
44. Huang L, Chen Y, Liu R, et al. P-glycoprotein aggravates blood brain barrier dysfunction in experimental ischemic stroke by inhibiting endothelial autophagy. *Aging Dis*. 2022;13(5):1546–1561. doi:10.14336/AD.2022.0225
45. He T, Shang J, Gao C, et al. A novel SIRT6 activator ameliorates neuroinflammation and ischemic brain injury via EZH2/FOXC1 axis. *Acta Pharmaceutica Sinica B*. 2021;11(3):708–726. doi:10.1016/j.apsb.2020.11.002
46. Bieber M, Gronewold J, Scharf AC, et al. Validity and reliability of neurological scores in mice exposed to middle cerebral artery occlusion. *Stroke*. 2019;50(10):2875–2882. doi:10.1161/STROKEAHA.119.026652
47. Wisniewski JR, Zougman A, Nagaraj N, Mann M. Universal sample preparation method for proteome analysis. *Nature Methods*. 2009;6(5):359–362. doi:10.1038/nmeth.1322
48. Liu R, Diao J, He S, et al. XQ-1H protects against ischemic stroke by regulating microglia polarization through PPARγ pathway in mice. *Int Immunopharmacol*. 2018;57:72–81. doi:10.1016/j.intimp.2018.02.014
49. An Y, Ni Y, Xu Z, et al. TRIM59 expression is regulated by Sp1 and Nrf1 in LPS-activated macrophages through JNK signaling pathway. *Cell Signalling*. 2020;67:109522. doi:10.1016/j.cellsig.2019.109522
50. Dobó J, Kocsis A, Farkas B, Demeter F, Cervenak L, Gál P. The Lectin Pathway of the complement system-activation, regulation, disease connections and interplay with other (proteolytic) systems. *Int J Mol Sci*. 2024;25(3). doi:10.3390/ijms25031566
51. Arumugam TV, Woodruff TM, Lathia JD, Selvaraj PK, Mattson MP, Taylor SM. Neuroprotection in stroke by complement inhibition and immunoglobulin therapy. *Neuroscience*. 2009;158(3):1074–1089. doi:10.1016/j.neuroscience.2008.07.015
52. Schartz ND, Tenner AJ. The good, the bad, and the opportunities of the complement system in neurodegenerative disease. *J Neuroinflammation*. 2020;17(1):354. doi:10.1186/s12974-020-02024-8
53. Dobó J, Kocsis A, Dani R, Gál P. Proprotein convertases and the complement system. *Front Immunol*. 2022;13:958121. doi:10.3389/fimmu.2022.958121
54. Van Beek J, Chan P, Bernaudin M, Petit E, MacKenzie ET, Fontaine M. Glial responses, clusterin, and complement in permanent focal cerebral ischemia in the mouse. *Glia*. 2000;31(1):39–50. doi:10.1002/(sici)1098-1136(200007)31:1<39::aid-glia40>3.0.co;2-1
55. Janiszewska E, Kmieciak A, Kacperczyk M, Witkowska A, Kratz EM. The Influence of Clusterin Glycosylation Variability on Selected Pathophysiological Processes in the Human Body. *Oxid Med Cell Longev*. 2022;2022:7657876. doi:10.1155/2022/7657876
56. Zong P, Li CX, Feng J, Yue L. Targeting TRPM2- and TRPM4-extrasynaptic N-methyl-D-aspartate receptor coupling in ischemic stroke. *Neural Regen Res*. 2023;18(11):2383–2384. doi:10.4103/1673-5374.371354